Bioorganic & Medicinal Chemistry 19 (2011) 3605–3615

Contents lists available at ScienceDirect

Bioorganic & Medicinal Chemistry

journal homepage: www.elsevier.com/locate/bmc

Computer- and structure-based lead design for epigenetic targets

Ralf Heinke [a], Luca Carlino [a], Srinivasaraghavan Kannan [a], Manfred Jung [b], Wolfgang Sippl [a,*]

[a] Department of Pharmaceutical Chemistry, Martin-Luther University of Halle-Wittenberg, 06120 Halle/Saale, Germany
[b] Institute of Pharmaceutical Sciences, University of Freiburg, 79104 Freiburg, Germany

ARTICLE INFO

Article history:
Received 2 October 2010
Revised 11 January 2011
Accepted 15 January 2011
Available online 22 January 2011

Keywords:
Epigenetic targets
Histone modifiers
Virtual screening
Inhibitor design
Docking

ABSTRACT

The term epigenetics is defined as inheritable changes that influence the outcome of a phenotype without changes in the genome. Epigenetics is based upon DNA methylation and posttranslational histone modifications. While there is much known about reversible acetylation as a posttranslational modification, research on reversible histone methylation is still emerging, especially with regard to drug discovery. As aberrant epigenetic modifications have been linked to many diseases, inhibitors of histone modifying enzymes are very much in demand. This article will summarize the progress on small molecule epigenetic inhibitors identified by structure- and computer-based approaches.

1. Introduction

The two major biochemical pathways of epigenetic regulation are DNA methylation and post-translational modifications of amino acids in histone proteins. The modifications interact with each other and constitute a particular pattern of alterations in the chromatin structure, the histone code.[1] Post-translational modifications of histones have been shown to participate in many cellular processes, including regulation of gene transcription and mitosis. Regulations of these covalent modifications, and the implications of this regulation, are currently of great interest in the scientific community.[2] Although histone proteins are subject to several post-translational modifications, such as acetylation, methylation, phosphorylation, ubiquitinylation or glycosylation, the focus of most studies has been so far mainly on lysine acetylation/deacetylation and methylation/demethylation. Over the years, many of the enzymes that regulate these histone modifications have been identified and characterized on a molecular level. A large effort has been accompanied by a wealth of 3D structures on epigenetic targets in an attempt to understand epigenetic targets and their regulation on a molecular level.[3] From the early discovery of histone deacetylase inhibitors, such as Trichostatin A, to the more recent discovery of other inhibitors of histone modifying enzymes, structure- and computer-based approaches were applied to analyze target–ligand interaction and to rationalize the development of small molecule modulators.[4] This review will summarize the progress on small molecule inhibitors identified by structure- and computer-based approaches that have been shown to modulate the activity of histone deacetylases, histone acetyltransferases, histone methyltransferases and histone demethylases.

1.1. Computer-based approaches

It has become common sense in drug discovery to use computer-based design techniques to identify and optimize novel molecules with a desired biological activity.[5] As a practical matter, computer-based methods are frequently divided into disciplines that focus on either structure-based or ligand-based approaches. When the 3D structure of a target protein is known, then it is possible to apply structure-based methods. New candidate molecules may be docked into a particular binding pocket in order to study if they can interact with the protein in an optimal way. In an ideal situation, the target protein has already been crystallized in complex with a first lead structure. However, in particular for novel targets, frequently structural information is not available at the time of the first experiments (e.g., high-throughput screening). If no 3D structure is available, but a sufficient number of active analogs have already been synthesized, then pharmacophore-based methods can be applied to identify novel molecules that fit a particular model.[6,7] It may seem straightforward to develop new molecules for known proteins by applying structure-based approaches, but significant problems are invoked. Protein flexibility, multiple ligand binding modes, solvation, or entropic effects are some of the problems that must be solved to end up with reliable models. There are also studies available that demonstrate the efficiency of ligand- and structure-based approaches in direct comparison,[6] as well as synergies obtained by using both approaches in

* Corresponding author. Tel.: +49 345 55 2540; fax: +49 345 55 27355.
E-mail address: wolfgang.sippl@pharmazie.uni-halle.de (W. Sippl).

0968-0896/$ - see front matter © 2011 Elsevier Ltd. All rights reserved.
doi:10.1016/j.bmc.2011.01.029

combination.[8] As the costs for computational power keep dropping and parallel computing is now available, theoretical modeling techniques are no longer a limiting problem to analyze large databases comprising millions of compounds.[5] In general, computer-based methods gained influence on the validation of targets, hit finding, hit to lead expansion, lead optimization, and also the prediction of suitable ADMET and off-target activity profiles.[9]

2. DNA methyltransferases

Only a few studies have been published so far where rational approaches have been used to identify selective inhibitors of DNA methyltransferases (DNMTs). One reason might have been the missing crystal structures of therapeutically relevant DNMTs, such as DNMT1. Due to the lack of an experimental 3D structure of DNMT1, Lyko and co-workers have generated a homology model for the catalytic domain based on the crystal structures of DNMT2 and bacterial homologues.[10] While this model demonstrated a significant conservation of the catalytic site—also due to the high sequence identity between the related enzymes (~50%)—it also revealed a number of unique structural features: His1459 of DNMT1 is substituted with alanine at the corresponding positions in the bacterial methyltransferases. In addition, the side chains of Arg1310 and Arg1312 have different conformations compared to the corresponding side chains in the two bacterial methylases. The authors stated that these differences influence the binding of the ribose ring in the cytosine ligand by creating a narrower cavity.

To identify small molecule DNMT inhibitors Siedlecki et al. screened the NCI Diversity Set using an in silico virtual screening approach (VS).[11] The Diversity Set consists of 1990 compounds that are representative of the chemical diversity of more than 140,000 compounds. To refine the database for docking calculations, unwanted compounds not suitable for the DNMT1 active site considering size, hydrophobicity, and uncommon atom types were removed. To test whether the applied scoring function is suitable for the DNMT binding pocket, known binders were used firstly as training set. The DOCK5[12] program was able to correctly predict the bioactive conformation of the training set ligands. The validated protocol was then applied to screen the NCI Diversity Set. The visual analysis of the docking and scoring data resulted in seven identified virtual hits. Two of them were experimentally tested in a cell-free in vitro assay and were found to be active in the range between 10 and 100 μM. The most interesting and most active compound is the tryptophan derivative **1** (RG108, NSC401077, Fig. 1). In the same study, compound **2** (NSC303530) was also identified as a somewhat weaker inhibitor. Analogues of **1** that do not contain the carboxylic acid group were found to be inactive.

Very recently a further VS study was reported from the same authors.[13] The screening focussed on a large database of natural products with a validated homology model of the catalytic domain of DNMT1. The VS focused on a lead-like subset of the natural products docked with DNMT1, using three docking programs, following a multistep docking approach. Consensus hits with high predicted docking affinity for DNMT1 by all three docking programs were identified. One hit showed DNMT1 inhibitory activity in a previous study. Further biological tests are necessary to confirm the derived hits.

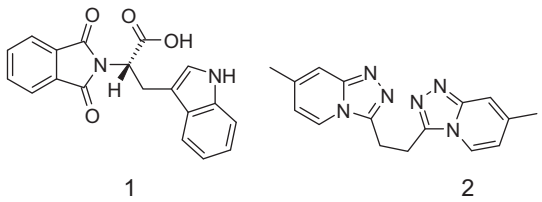

Figure 1. Molecular structures of two DNMT inhibitors identified by VS of the NCI diversity set.[11]

3. Histone deacetylases

3.1. Classical (zinc dependent) HDACs

So far 18 different HDACs have been discovered in humans and have been classified into four classes based on their homology to yeast histone deacetylases.[14] Class I includes four different subtypes (HDAC1, 2, 3 and 8), class II contains six subtypes which are divided into two subclasses, class IIa with subtypes HDAC4, 5, 7 and 9, and class IIb with HDAC6 and 10. Class I and class II HDACs share significant structural homology, especially within the highly conserved catalytic domains. HDACs 6 and 10 are unique as they have two catalytic domains. HDAC11 is referred to as class IV. While the activity of class I, II and IV HDACs depends on a zinc based catalysis mechanism, the class III enzymes, also called sirtuins, require nicotinamide adenine dinucleotide as a cofactor for their catalysis (see below).

Cocrystal structures of HDACs in complex with hydroxamic acid containing ligands have been useful in dissecting the molecular details of HDAC inhibition.[15] The first of these structures was obtained with HDAC-like protein (HDLP) complexed with two different inhibitors.[4] Later, crystal structures of human HDAC2, HDAC4, HDAC7 and HDAC8, as well as bacterial FB188 HDAH have been resolved.[3] Unfortunately, for two of the most promising HDAC subtypes for drug discovery, HDAC1 and HDAC6, no structural data is available at the moment. The architecture of the solved HDACs is very similar, with the residues in the active site being conserved between bacterial and human HDACs. However, the organization of the loop and distal helices is different in the known HDAC structures, for example, HDAC8 shows a more open and accessible substrate binding channel. The deacetylase active site with the zinc ion is located at the end of an approximately 12 Å long tunnel. The zinc ion is penta-coordinated by two aspartic acids and one histidine. The rest of the substrate channel is made up of lipophilic amino acids which are highly conserved across the isoforms. Especially, two aromatic side chains which restrict the width of the tunnel can be found at the same position in the different HDAC structures. At the top of the binding cavity a rim

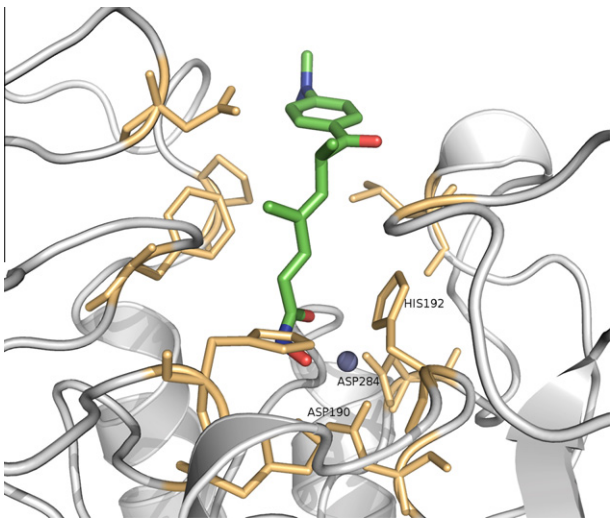

Figure 2. Crystal structure of HDAC7 (3C10.pdb) in complex with the inhibitor Trichostatin A (green carbons). Only the residues in the binding pocket are shown. The zinc ion is shown as blue colored ball.

is leading to the surface, which is formed by several loop regions that differ between subtypes. As an example the binding mode of the cocrystallized inhibitor Trichostatin A (**3**) with HDAC7 is shown in Figure 2.

In the crystal structures, the inhibitors coordinate to the active site zinc and make a series of hydrogen bonds via their hydroxamic acid moiety. The hydroxamic acids are linked by a flexible spacer with bulky cap groups. The aromatic or aliphatic spacer participates in Van der Waals-interactions throughout the long channel, whereas the terminal part of the inhibitor interacts with residues at the rim of HDAC. In general, the binding mode of the cocrystallized inhibitors **3** and **4** (SAHA, Vorinostat) is conserved among the different species and subtypes.[16] The recently solved crystal structure of HDAC2 in complex with a benzamide derivative, showed for the first time that the aniline and amide group of this inhibitor class can also be coordinated to the zinc-ion.[17] (Fig. 3) Thus, the binding mode for well known inhibitors such as **5** (MS-275) is now better understood.

3.2. Docking studies using X-ray structures and homology models

Ligand bound structures of the target protein provide a suitable starting point for structure-based drug design. Since the first of the solved structures was that of HDLP, molecular modeling studies started with the analysis of the inhibitor binding mode for this bacterial enzyme. A variety of studies were reported in the meantime where structure-based optimization of HDAC inhibitors was successfully guided by docking the compounds into the HDLP active site.[18–28] In the case of HDAC1 and HDAC6 a crystal structure of the enzyme is yet to be elucidated and in its absence, homology models of HDAC-1 and HDAC-6 complexed with hydroxamate based inhibitors were generated by several groups.[29–40] The refined models were generally checked for structural integrity using molecular dynamics simulations and various protein structure checking tools. The predictive ability of the models was evaluated through docking studies of known hydroxamate or benzamide based HDAC inhibitors. For constructing the homology models the available crystal structures of HDLP and HDAC8 were considered in case of HDAC1. The models show a high degree of similarity compared to the HDAC8 crystal structure. The two conserved aromatic amino acids (Phe150 and Phe205 in case of HDAC1) face each other and form the narrowest part of the substrate channel. The channel exit is composed of non-structured loop regions. Molecular dynamics simulations have indicated a high flexibility of this region, which makes structure-based design a challenging task.[41] For HDAC6, which has two catalytic domains, so far only two 3D models have been reported. Whereas one was generated on the basis of the bacterial FB188 HDAH (38% sequence identity)[42] a further model was derived using the recently published human HDAC7 crystal structure in complex with **3** and **4** (49% sequence identity).[37] Both HDAC6 models were generated for the catalytic domain located at the C-terminal region and have been used to explain structure–activity relationships for a series of HDAC6-selective inhibitors. In the study by Schäfer et al.[37,43] the generated HDAC6 model was used to dock a series of biaryl- and pyridylalanine containing hydroxamate inhibitors. A clearly defined hydrophobic binding cavity was proposed that is formed by several aromatic and hydrophobic residues (His499, His560, Phe566, and Ile569) which accommodate the hydrophobic cap group of the inhibitors.

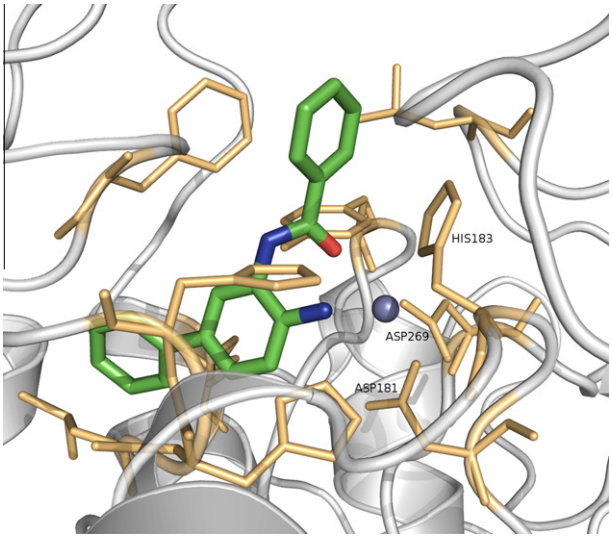

Figure 3. Crystal structure of an HDAC2-inhibitor complex (3MAX.pdb). The aniline nitrogen as well as the amide oxygen atoms of the inhibitor (green carbons) are chelating the zinc ion of the catalytic site. The second aromatic ring is interacting at a foot pocket identified in the HDAC2 protein structure. The zinc ion is shown as blue colored ball.

3.3. 3D-QSAR studies

QSAR[44–46] and 3D-QSAR[47–51] models for HDAC inhibitors were used to explain the differences in activity of certain hydroxamate-based compounds. All the reported models, which showed moderate to good internal predictivity, were mainly used retrospectively to explain the biological activities of HDAC inhibitors. Generally, the 3D-QSAR models were compared with ligand docking results to get insight into the structural requirements for HDAC inhibition.

3.4. Virtual screening studies

High-throughput screening of chemical libraries is a well-established method for finding new lead structures in early drug discovery. However, the increasing number of purchasable compounds makes fast and reliable pre-filtering methods necessary to reduce the number of compounds selected for experimental testing. In contrast to high-throughput screening, in VS compounds are selected on the basis of computer-based prediction. In this way, VS approaches try to select the most promising compounds from supplier/in-house databases for biological testing. VS can be carried out by applying different approaches: by searching databases for molecules with chemical similarity to a set of known actives,[52] by identifying compounds which match a given pharmacophore,[5] or by fitting molecules into the three-dimensional structure of a macromolecular target.[53] In addition, pre-screening filters are usually applied that filter out compounds with potentially poor pharmacokinetic properties or unwanted chemical reactivity. The secret to success in VS lies in the choice of an appropriate combination of methods.[54,55]

To evaluate the performance of a given VS technique, validation studies are usually carried out. For this purpose, known binders are pooled with a set of randomly selected compounds (called decoys) to assess how well the known binders 'enrich' during the course of the screening process. There is a big debate as to how similar the decoys should be to the active molecules and what the ratio of actives and decoys should be.[56–59] Such considerations are relevant for the development of new methods; however, in actual drug discovery projects, at the end of the day, a newly discovered chemotype or a drug-like lead structure represents the ultimate goal. Impressive enrichment rates of known actives will not be convincing when it is easy to separate them from the decoys solely on simple 1D descriptors such as molecular weight or protonation

state.[55] For that purpose some guidelines are given in the literature how to assemble a right decoy set.[57] Since the early VS attempts, a plethora of application studies has been performed and the list of success stories is steadily growing. Despite the fact that VS is still a developing discipline, it has been reviewed frequently,[9,53,60,61] most recently in comprehensive overviews.[54,55,62]

Only a few VS studies focussing on HDACs have been published so far. The rationale for that might be the yet unsolved crystal structure of the therapeutically interesting subtypes HDAC1 and HDAC6 and the limited number of commercially available hydroxamates. At Argenta, a VS approach was initiated based on the published crystal structure (PDB code: 1C3R) of the HDAC-like protein (HDLP).[63] A virtual library of 644 hydroxamic acids was generated from a database of available carboxylic acids. The designed compounds, were docked and scored using the FlexX program.[64] Based on the VS results, 75 compounds were selected and tested in an HDAC (subtype) enzyme assay. Compound **6** (ADS100380, Fig. 4) was identified as a submicromolar (IC_{50} = 0.75 μM) HDAC inhibitor. As expected, the corresponding carboxylic acid of **6** was inactive. The docking study indicated that the catalytic zinc ion to which the hydroxamic acid group of **6** binds is located at the bottom of a tube-shaped pocket. Thus, optimization of **6** was designed to make additional interactions at the entrance to the HDAC active site by tethering hydrophobic aromatic groups to the pyrazole nitrogen. Several nanomolar HDAC inhibitors were obtained by the structure-guided optimization process (e.g., inhibitor **7** in Fig. 4).

Very recently, a VS study was reported which was able to identify a novel class of HDAC inhibitors.[65] Park et al. docked ~180,000 molecules from the InterBioScreen database into homology model of HDAC1. The model had been validated by docking known inhibitors of HDAC1 into the model structure. The authors were able to identify six novel HDAC inhibitors with IC_{50} values in the low micromolar range using the commercially available BIOMOL HDAC fluorescence assay.[65] Interestingly, these inhibitors contain zinc-chelating groups not previously reported for HDAC inhibitors, including the *N*-[1,3,4]thiadiazol-2-yl-sulfonamide group (compounds **8**–**10**, Fig. 5). By analyzing the docking poses it was observed that the nitrogen atom of the heterocycle and one of the sulfonamide oxygen atoms are coordinating to the zinc ion of HDAC. The most active compound **8** with an IC_{50} value of 4.3 μM is shown in Figure 5.

A variety of retrospective VS studies have been published where ligand- and pharmacophore-based models have been tested to identify already known HDAC inhibitors among randomly selected decoys.[66–68] The models were shown to be able to discriminate active HDAC inhibitors from other molecules. Unfortunately no experimental validation of the novel identified compounds was carried out, thus making it impossible to evaluate the general value of these approaches.

3.5. Sirtuins

The class III deacetylases, named sirtuins, are structurally and functionally different from other HDACs. In contrast to the zinc-dependent deacetylation of classical HDACs, sirtuins depend on NAD^+ to carry out catalytic reactions. A variety of sirtuin crystal structures have been published over the last few years (for a recent review see[69]). The structures of human Sirt2, Sirt3 and Sirt5, as well as several bacterial Sir2 proteins could be derived whereas no 3D structure is available for Sirt1.[70] All solved sirtuin structures contain a conserved 270 amino acid catalytic domain with variable N- and C-termini. The structure of the catalytic domain consists of a large classical Rossmann-fold and a small zinc binding domain. The interface between the large and the small subdomain is commonly subdivided into A, B and C pocket. This division is based on the interaction of adenine (A), ribose (B) and nicotinamide (C) which are parts of the NAD^+ cofactor. (Fig. 6) Whereas the interaction of adenine and ribose is similar in all available sirtuin X-ray structures, the interaction of the nicotinamide part is less clearly defined. Several, so called productive and non-productive, conformations of nicotinamide have been observed in the crystal structures, reflecting the high flexibility of this part of the cofactor. In the X-ray structure of a Sirt2 homologue from Archeabacteria it was shown that the acetylated peptide binds in a cleft between the two domains.[71] The acetyl-lysine residue inserts into a conserved hydrophobic pocket, where NAD^+ binds nearby (Fig. 6). In case of the human Sirt2 X-ray structure no structural information about the NAD^+ or substrate binding is available. However, due to the homology with bacterial sirtuins, docking studies showed that NAD^+ interacts in a comparable way with human and bacterial enzyme.[72]

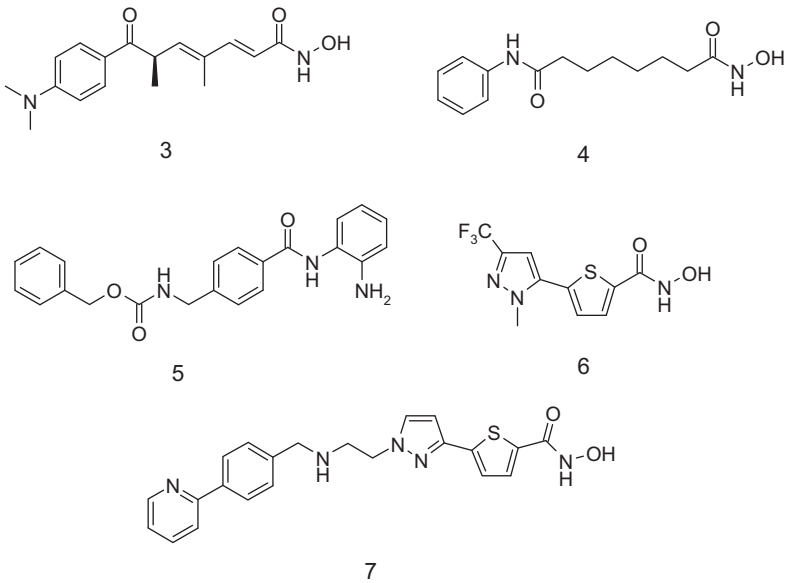

Figure 4. Molecular structures of HDAC inhibitors mentioned in the text.

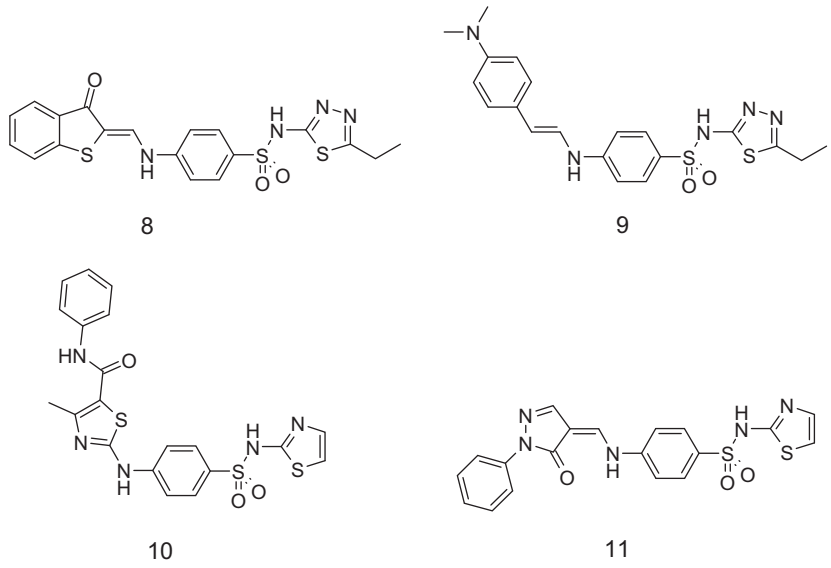

Figure 5. Molecular structures of sulfonamides identified as HDAC inhibitors by virtual screening.

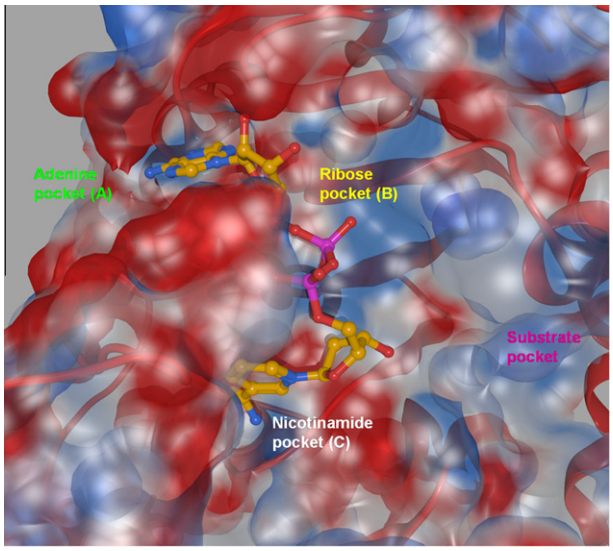

Figure 6. X-ray structure of human Sirt2 in complex with NAD^+ (predicted by docking). The molecular surface of the protein is colored according to the electrostatic potenital (red = negative potential, blue = positive potential).

Several inhibitors are available for Sirt2 that have been discovered by VS approaches.[73–75] Based on docking studies that were carried out for human Sirt2 and competition experiments with NAD^+ it was found that adenosine mimetics (e.g., the kinase inhibitor **11**, Ro-318220, Fig. 7) are potent Sirt2 inhibitors (IC_{50} 0.4 μM) which interact with the adenine sub-pocket.[74] The planar ring system of the docked inhibitor **11** fits perfectly in the adenine-binding pocket and makes hydrogen bonds with Cys324 and Asp325. A second putative binding site for the polar amidine group of Ro-318220 was observed at the polar ribose binding site near Ile93 and Asp95.

Tervo et al. carried out a receptor-based VS on the screening collection from Maybridge comprising about 60,000 compounds.[75] Using the UNITY software[76] a simple pharmacophore query was generated first to select potential Sirt2 hits. The database searching returned 66 candidate compounds, of which 44 compounds passed an in silico intestinal absorption model generated with the VOLSURF program.[77] The retrieved hits were subsequently docked in the Sirt2 binding pocket using the GOLD program.[78] The location of the docking poses at the active site, as well as their ability to match the requirements of the search queries, was visually analyzed. On the basis of the visual inspection, 15 compounds were selected in order to test their ability to inhibit Sirt2 in vitro. Two out of 15 experimentally tested compounds showed a moderate in vitro inhibitory activity toward Sirt2 (**12**, JFD00244 IC_{50} 57 μM and **13**, CD04097 IC_{50} 74 μM; Fig. 7). The docking study which was carried out with the human Sirt2 crystal structure revealed that the active inhibitors interact mainly with Asp95, Gln167, Asn168, and with Ile169, mostly by forming hydrogen bonds to the backbone atoms. On the basis of the docking study, the authors suggested that this region, which is also the postulated binding site for nicotinamide, is also important for the inhibitor binding. This observation is also supported by the finding that the docked inactive compounds don't show hydrogen bonds to these amino acid residues. Using the same approach Poso et al. performed further VS on other compound libraries.[79–81] Several moderately active inhibitors could be identified from the Leadquest and Maybridge compound collections.

A recent effort to identify a Sirt2 inhibitors culminated in the report of the vinylnitrile **14** (AGK2, Fig. 7). Compound **14** and chemically similar analogs were identified in a focussed library screening. To elucidate the structural mechanism of Sirt2 inhibition by **14** Outeiro et al.[82] developed 3D models of human Sirt2 in several different conformations by combining available human and yeast crystal structures. The high flexibility of the active site loop made this strategy necessary. The different Sirt2 conformations were subsequently used for docking the identified inhibitors using the ICM program.[83] Comparative analysis of the low energy ligand conformations confirmed that the preferred site for ligand binding is the pocket C where the nicotinamide part of NAD^+ is interacting. A hydrogen-bonding pattern for **14** was observed which is similar to that of other Sirt2 inhibitors. **14** inhibits Sirt2 with an IC_{50} value of 3.5 μM and shows more than ten-fold selectivity versus Sirt1 and Sirt3. In further biological experiments compound **14** displayed the ability to block α-synuclein-mediated toxicity in a Parkinson's disease model, possibly by modulating tubulin acetylation.

Neugebauer et al. used docking simulations to analyze the binding of several Sirt2 inhibitors and to rationalize the structure–activity relationships of a series of developed arylsplitomicins (**15**, Fig. 7).[84] Docking studies using the human Sirt2 X-ray

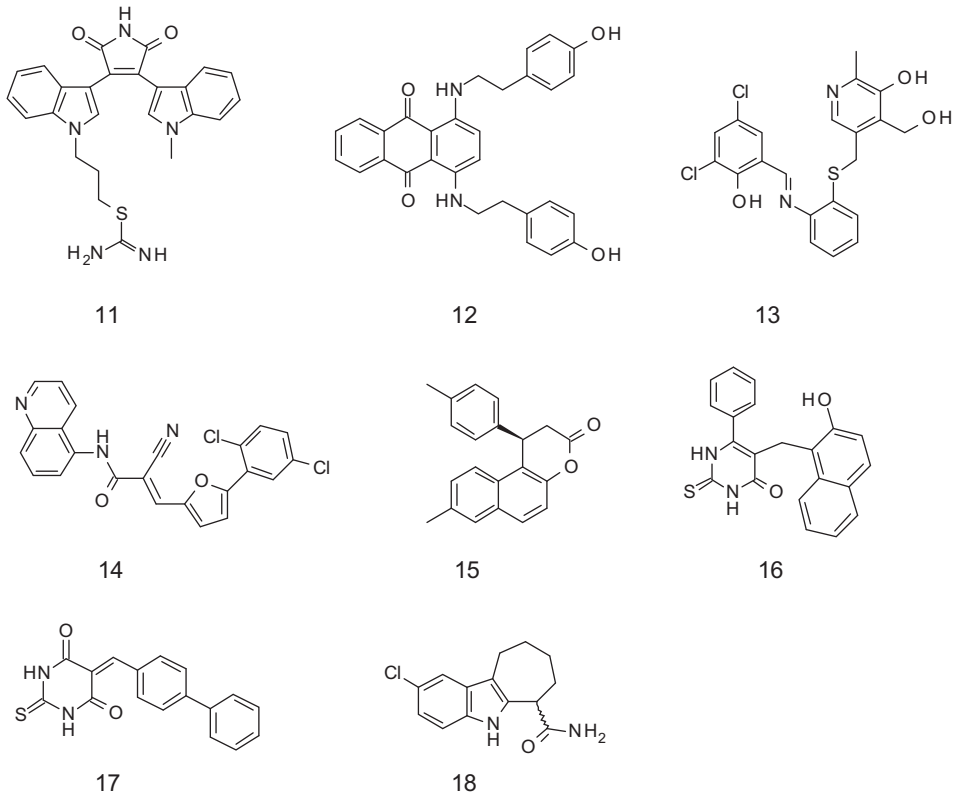

Figure 7. Molecular structures of sirtuin inhibitors mentioned in the text.

structure showed that the known Sirt2 inhibitor cambinol (**16**) as well as the active arylsplitomicin (**15**, Fig. 8) interact with the nicotinamide subpocket (C). By synthesizing and assaying the pure enantiomers of the β-phenylsplitomicin **15** (Fig. 7) the postulated binding mode could be validated. As predicted by the docking study only the (*R*)-isomer is a potent Sirt2 inhibitor with a IC_{50} of 1.0 μM whereas the (*S*)-isomer is weakly active. A similar binding mode was later observed by synthesizing and docking cambinol analogs[85] which were predicted to interact with the same subpocket C.

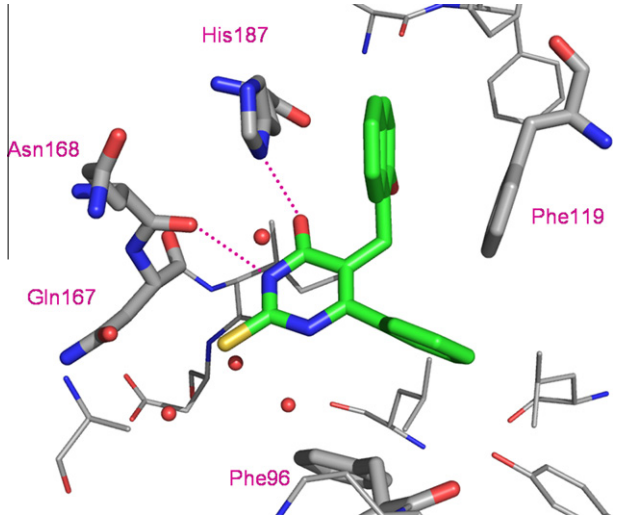

Figure 8. Binding mode of **16** (green carbons) at the Sirt2 binding pocket. Hydrogen bonds are shown as dashed line.

VS of commercial databases and subsequent docking the hits into the Sirt2 binding site yielded a novel class of inhibitors containing a thiobarbiturate structure, which shows similarity to the cambinol structure.[86] A set of seven active Sirt1 and Sirt2 inhibitors could be identified and the binding mode was predicted using the GOLD docking program. To rationalize the experimental results, binding free energy calculations were carried out by molecular mechanics Poisson-Boltzmann/surface area (MM-PBSA) calculations.[87] A significant correlation between calculated binding free energies and measured Sirt2 inhibitory activities was observed. Thus, the prediction model could be used to estimate the inhibitory activity of novel candidate drugs. The analyses suggested a molecular basis for the interaction of the identified thiobarbiturate derivatives with human Sirt2. The interaction of the most potent thiobarbiturate **17** (IC_{50} 8.7 μM) with human Sirt2 is shown as an example in Figure 9. A common feature of the active inhibitors is the interaction (hydrogen bond) of one thiobarbiturate NH-group with the backbone carbonyl of Gln167 and the hydrogen bond between the barbiturate CO-group and His187. The bulky naphthyl or biaryl substituent is facing in the acetyl-lysine substrate channel and makes van der Waals interactions with the aromatic ring system of Phe119 and His187.

The available structural information on human sirtuins and the derived docking results suggest that inhibitors can interact with different binding pockets. Whereas for adenosine analogs an interaction was predicted for the adenine pocket and verified by competition experiments, for a variety of inhibitors (e.g., **14**, β-phenylsplitomicin **15**, cambinol **16**, thiobarbiturate **17**, and the indole **18**) bearing polar moieties the interaction with the nicotinamide or the substrate pocket is postulated. Crystal structures of human sirtuins together with inhibitors from the different structural classes will be helpful for the structure-based optimization.

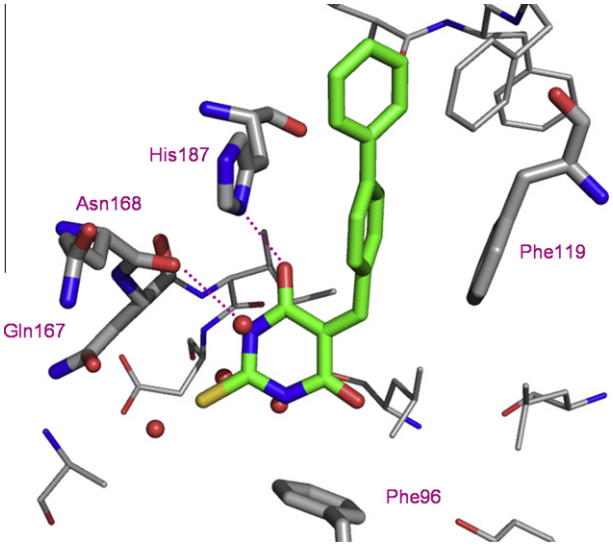

Figure 9. Interaction of the thiobarbiturate **17** (green carbons) with the Sirt2 binding site. Hydrogen bonds are shown as dashed line.

4. Histone acetyltransferases

Histone acetyltransferases (HATs) enzymes have been divided into several families based on conserved sequence motifs. The two major families are named GNAT (Gcn5-related N-acetyltransferases) and MYST (MOZ, Ybf2/Sas3, Sas2, Tip60). Numerous structural studies have been carried out on HATs in the last decade that lead to a wealth of structural data on the GNAT, MYST and p300/CBP families.[88–90] Despite the large number of available crystal structures derived for HATs, HAT-cofactor and HAT-substrate complexes, only one study was reported so far which used the 3D structural information for VS or molecular design of HAT inhibitors.[91]

Bowes et al. docked 500,000 molecules into the p300 HAT crystal structure using the ICM docking program[83] and biologically tested 194 selected hits coming out of the VS. Among the actively tested compounds (Fig. 10) the pyrazolone-containing small molecule p300 HAT inhibitor **19** was identified. **19** was shown to be a competitive p300 inhibitor with an K_i of 400 nM and was found to be selective versus other acetyltransferases. In addition, two further moderately active inhibitors (**20, 21**, Fig. 10) were identified. Studies on site-directed p300 HAT mutants and synthetic modifications of **19** confirmed the predicted binding mode and the importance of particular interactions in conferring potency. The other few available HAT inhibitors were mostly identified by random screening campaigns or empirical findings.[92]

5. Histone methyltransferases

During the past several years, a variety of crystal structures of histone lysine and arginine methyltransferase in complex with the cofactor analog *S*-adenosyl-L-homocysteine (SAH) and/or in complex with peptide substrates have been reported.[93] However, only one three-dimensional structure of a complex between a histone methyltransferase (HMT) and an inhibitor has been reported so far.[94]

Due to the lack of experimental structures a variety of molecular modeling and docking studies has been carried out for HMTs in order to understand the structural requirements for inhibitor binding.

The first crystal structure for a PRMT enzyme was reported in 2000 for rat PRMT3 in complex with the cofactor analogue SAH.[95] The results revealed a two-domain structure—a SAH binding domain and a barrel-like domain—with the active site pocket located between the two domains. The rat PRMT1 crystal structure in complex with SAH and a substrate peptide were published in 2003 and allowed for the first time the analysis of the enzyme–substrate interaction.[96] Mutagenesis studies on rat PRMT1 confirmed that two active site glutamate residues (Glu144 and Glu153) are essential for enzymatic activity, and that dimerization of PRMT1 is essential for cofactor binding. The crystal structures of rat PRMT1 were obtained at a non-physiological pH-value (pH 4.7; maximum enzymatic activity at pH 8.5), resulting in a conformational change of one of the active site glutamates (Glu153) and a disordered helix αX which is part of the substrate binding pocket.

The available rat PRMT1 and PRMT3 crystal structures have been used to provide a structural explanation for the inhibitory activity of a set of synthesized analogues of eosin (**22**, Fig. 11). Docking of inhibitors such as **23** (Fig. 11) into PRMT1 and the *Aspergillus* homologue RmtA revealed a potential interaction with the arginine substrate and the cofactor binding pocket. In contrast, related analogs could be docked either in the cofactor or substrate binding site. However no experimental confirmation by competition experiments has been reported to support the postulated binding mode.[97] The reported series of dye-related small molecules was further used to establish a receptor-based 3D QSAR model for nine selected inhibitors from the study. The 3D QSAR model which was generated using the GRID/GOLPE[98] approach showed good internal predictivity (q^2 = 0.93). However, due to the limited number of molecules in the 3D QSAR analysis, the model is of limited validity.

In a further study Mai et al.[99] have chosen the eosin (**22**, Fig. 11) chemical structure as a template to design a new series of simplified analogues starting from a pharmacophore hypothesis. In this hypothesis, the presence of two *o*-bromo- or *o*,*o*-dibromophenol moieties inserted into hydrophobic moieties were identified as

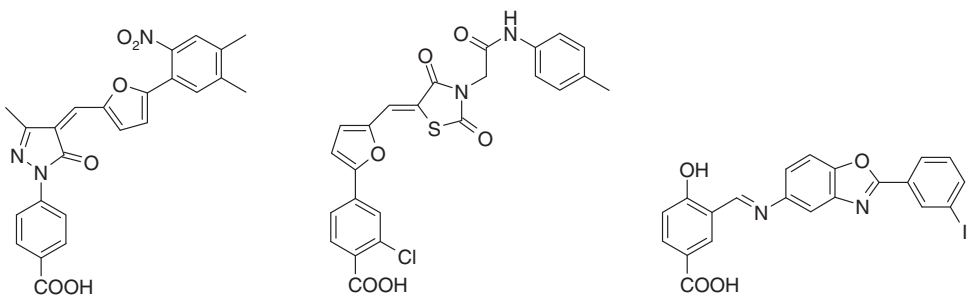

19 20 21

Figure 10. Molecular structures of HAT p300 inhibitors identified by virtual screening.

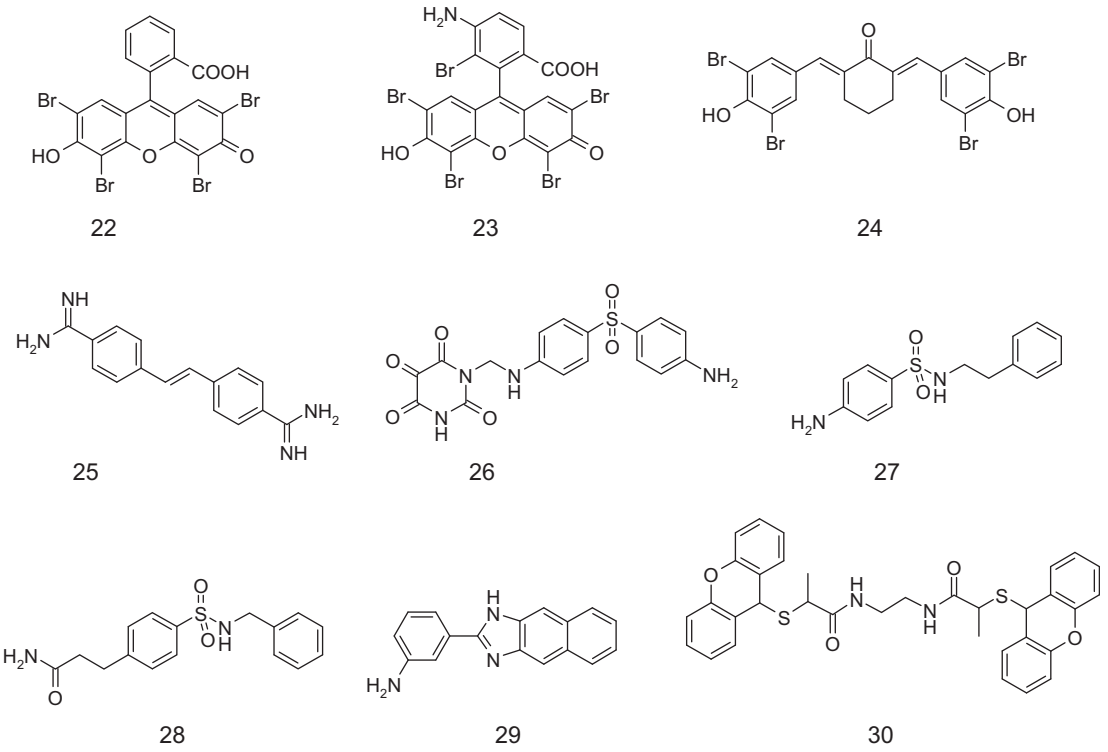

Figure 11. Molecular structures of PRMT inhibitors mentioned in the text.

crucial for having antimethyltransferase activity. They prepared a series of substituted 1,5-diphenyl-1,4-pentadien-3-ones (e.g., compound **24** Fig. 11) and docked them into the generated model structures of human PRMT1, CARM1 and into the SET7 crystal structure. The analysis of the AutoDock-proposed binding modes revealed that the compounds are able to bind in the SAM or in the Arg/Lys substrate binding sites. The most active compounds could be docked in the SAM binding pocket of the two PRMTs (PRMT1 and CARM1), whereas for SET7, most of the developed compounds occupied both the lysine and cofactor binding sites.

Applying a combination of structure-based VS and biochemical characterization two drug-like substrate competitive PRMT1 inhibitors (**25**, stilbamidine and **26**, allantodapsone, Fig. 11) have been reported recently.[100] Based on a generated homology model of human PRMT1 and subsequent docking into the substrate binding site, key interactions between the identified inhibitors and PRMT1 could be derived. A common feature of the actively tested inhibitors is the hydrogen bonding of a basic or polar group with the active site Glu152 (which corresponds to Glu144 in rat PRMT1). A basic or polar moiety of the inhibitors mimics the guanidine group of the arginine side chain of the substrate peptide. In addition, the inhibitors show van der Waals interactions with several aromatic residues of the binding pocket (Tyr47, Tyr156, Trp302) (Figs. 12A and 12B). The proposed binding mode could be confirmed by competition experiment using a synthetic histone substrate.

Based on the identified PRMT1 inhibitor **26**, Heinke et al.[101] expanded their virtual and biological screening for novel inhibitors. Structure-based VS of the Chembridge database comprising 328,000 molecules was performed using a combination of ligand- and target-based in silico screening. 189,000 molecules were screened in silico using a structure-based pharmacophore model generated with the program LigandScout. Subsequently docking the compounds which passed the pharmacophore and analyzing the top-ranked hits nine compounds from clusters of similar molecules were selected and experimentally tested using human

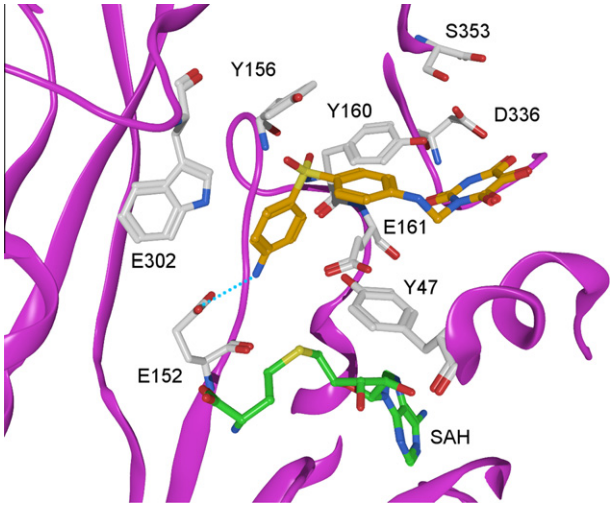

Figure 12A. Predicted binding mode of **25** (colored magenta) at the substrate binding pocket of PRMT1. The cofactor analog SAH is shown in orange at the bottom of the figure. Hydrogen bonds are shown as dashed lines. Only residues of the binding site are displayed.

PRMT1 and an antibody based assay with a time-resolved fluorescence readout (**27–29**, Fig. 11). Among several aromatic amines (**27** and **29**) also an aliphatic amine and an amide (inhibitor **28**) were found to be active in the μM range.

A further fragment-based VS identified α-methylthioglycolic amides as new lead PRMT inhibitors. Similarity based searching for analogues resulted in inhibitor **30** (Fig. 11), which was identified as bisubstrate PRMT1 inhibitor. Docking of **30** showed that the compound blocks the cofactor and the substrate channel showing mainly favorable van der Waals interaction with aromatic residues (Tyr43, Tyr47, Met56, Val108, Tyr156, Tyr160) of the cofactor and Arg-binding pocket.[102]

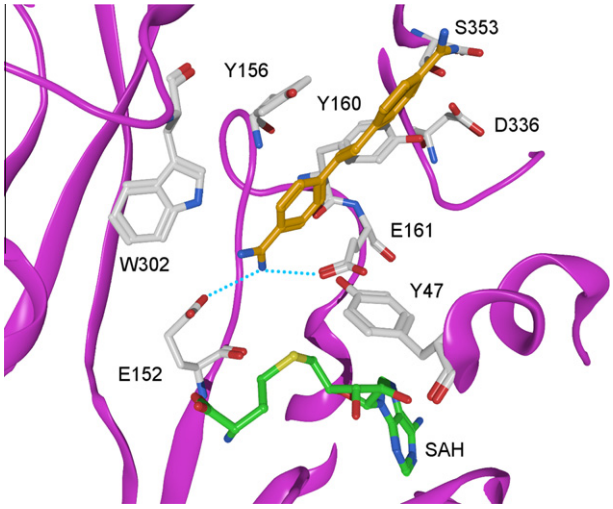

Figure 12B. Predicted binding mode of **26** (colored magenta) at the substrate binding pocket of PRMT1. The cofactor analog SAH is shown in orange at the bottom of the figure. Hydrogen bonds are shown as dashed lines. Only residues of the binding site are displayed.

Kubicek et al. applied both VS and HTS to screen the Boehringer Ingelheim chemical compound library for inhibitors of the lysine methyltransferase G9a. Cheminformatic tools were used to identify molecules that would have an increased probability to function as potential G9a inhibitors.[103,104] The similarity was calculated on the basis of ligand/protein-based fingerprints/site-points.[105] The approach was used both for a ligand-based and protein-based VS. For the protein-based screening a homology model based on the crystal structure of DIM-5 (1PEG.pdb),[106] a lysine methyltransferase with 30% identity in the SET domain to G9a, was developed. Each method scored the compounds in the screening collection. Additional compounds were randomly selected, and a total of 125,000 substances were subsequently evaluated in HTS. The experimental in vitro testing on G9a revealed seven hits with activities in the low micromolar range. Beside the unselective inhibitor acylbenzimidazole **31** (BIX-01338), the selective inhibitor **32** (BIX-01294) was identified (Fig. 13). Compound **32** inhibited G9a at 2.7 μM (IC_{50}) and did not show activity against SUV39H1 or PRMT1.

The predicted binding mode of **32** could be confirmed recently by the crystal structure of the catalytic SET domain of the G9a-like protein GLP (which is a close homologue of G9a) in complex with the inhibitor and the cofactor analog SAH.[94] **32** was shown to bind in the substrate peptide groove at the location where the histone H3 residues N-terminal to the target lysine lie in the previously solved structure of the complex with a histone peptide. The co-crystallized inhibitor resembles the bound conformation of histone H3 Lys4 to Arg8, and is positioned in place by residues specific for these lysine methyltransfereases through specific interactions (Fig. 14A).

The available crystal structure of **32** in complex with GLP has been used to carry out structure-guided optimization of this inhibitor family. The X-ray crystal structure of the complex revealed that **32** occupied the histone peptide binding site and did not interact with the narrow lysine binding channel. The authors hypothesized that adding a 7-aminoalkoxy side chain to the quinazoline scaffold would make new interactions with the lysine binding channel while the rest of molecule maintained interactions with the peptide binding groove. The new compound **33** (UNC0224) (Fig. 13) was found to be 7-times more potent (IC_{50} 15 nM at G9a) compared to the parent compound (IC_{50} 106 nM).

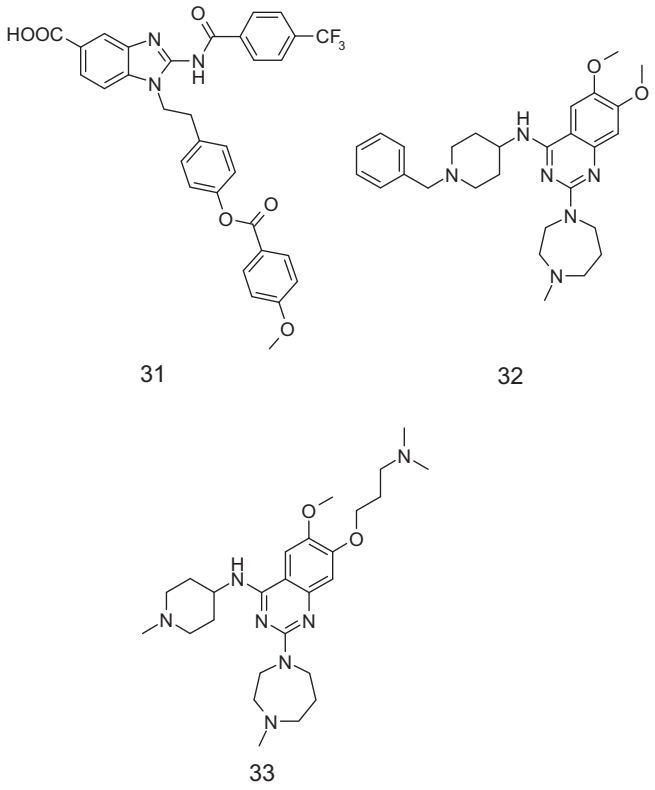

Figure 13. Molecular structures of G9a inhibitors mentioned in the text.

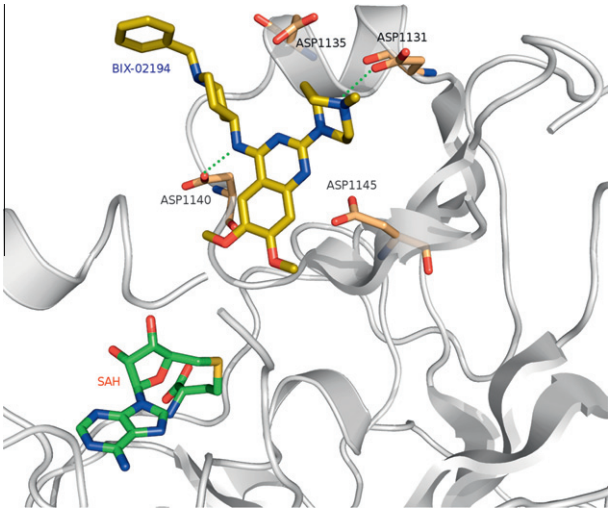

Figure 14A. Crystal structure of the GLP methyltransferase (3FPD.pdb) in complex with the inhibitor **32** (colored yellow). The inhibitor is involved in two hydrogen bonds to D1131 and D1140. (The cofactor analog SAH is colored green and the protein backbone is shown as purple ribbon. Only interacting residues of GLP methyltransferase are displayed).

The interaction of **33** with the enzyme could be verified by solving the crystal structure of the inhibitor bound to GLP (Fig. 14B). As predicted, it was found that the 7-dimethylaminopropoxy side chain of **33** indeed occupied the lysine binding channel of G9a nicely, thus validating the binding hypothesis. Thus, the higher potency of **33** compared to **32** was explained by an additional interaction between the 7-dimethylaminopropoxy side chain and the lysine binding channel.

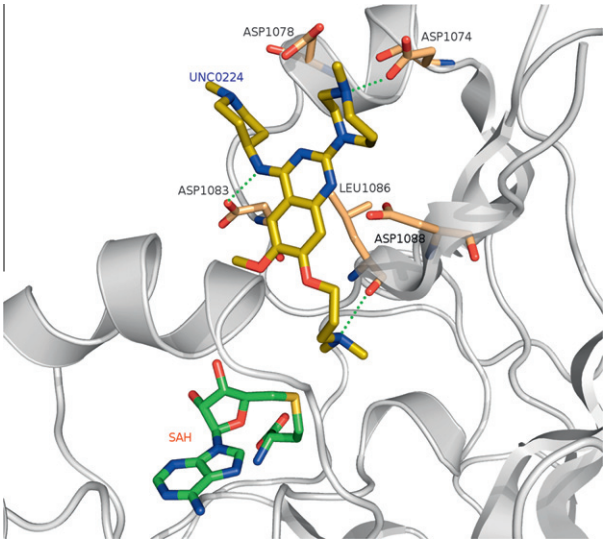

Figure 14B. Crystal structure of the G9a methyltransferase (3K5K.pdb) in complex with inhibitor **33** (colored green). Same coloring scheme is used as in Figure 14A.

6. Histone demethylases

The first histone demethylases (HDMs) have been identified only recently. In 2004, Shi and co-workers discovered the first demethylase specifically demethylating histone H3 at lysine 4 and named it LSD1 (lysine-specific demethylase-1).[107,108] LSD1 shows a high sequence homology with FAD-dependent amine oxidases. Two years later, another family of histone demethylases was identified and termed JmjC protein.[109] These demethylases use Fe(II) and α-ketoglutarate in an oxygenation reaction to remove the methyl groups from lysine residues. Since the expression levels of several of these demethylases are increased in primary tumors, HDMs are considered as potential drug targets.[110] Therefore it is not surprising that a huge effort is now made to explore the structural requirements of modulating these targets and to identify small molecule inhibitors. A variety of crystal structures have been solved in the last four years which helped in understanding the binding of substrates and first available unselective inhibitors.[111,112] It is likely that the available 3D structures of HDMs will soon result in the structure-guided design of druglike and selective inhibitors.[113]

7. Summary

Despite many technical challenges, structure-based VS has an important role in drug discovery. As a steadily growing number of epigenetic targets are characterized biologically and also structurally, structure-based methods are more and more applied to design specific inhibitors to elucidate their therapeutic potential. Ligand docking and scoring technologies have steadily improved and the importance of the adequate validation of pragmatic VS protocols is now well recognized. While both ligand- and receptor-based approaches already have demonstrated their value in identification of novel lead compounds for epigenetic targets, there is still the challenge to improve the predictive accuracy of scoring functions, particularly to enable scoring-based methods to have a greater impact in guiding lead optimization.

Acknowledgements

Financial funding by the DFG (SI 868/4-1, and /6-1, JU 295/7-1 and /8-1, Dr. Mildred Scheel Stiftung/Deutsche Krebshilfe (Nr. 107898) and EU (SEtTReND) is acknowledged.

References and notes

1. Wolffe, A. P.; Matzke, M. A. *Science* **1999**, *286*, 481.
2. Kouzarides, T. *Cell* **2007**, *128*, 693.
3. Romier, C.; Wurtz, J. M.; Renaud, J. P.; Cavarelli, J. *Epigenetic Targets in Drug Discovery*; Wiley-VCH Verlag GmbH & Co. KGaA, 2009. pp 23–56.
4. Finnin, M. S.; Donigian, J. R.; Cohen, A.; Richon, V. M.; Rifkind, R. A.; Marks, P. A.; Breslow, R.; Pavletich, N. P. *Nature* **1999**, *401*, 188.
5. Kirchmair, J.; Distinto, S.; Schuster, D.; Spitzer, G.; Langer, T.; Wolber, G. *Curr. Med. Chem.* **2008**, *15*, 2040.
6. Hawkins, P. C. D.; Skillman, A. G.; Nicholls, A. *J. Med. Chem.* **2006**, *50*, 74.
7. Evers, A.; Hessler, G.; Matter, H.; Klabunde, T. *J. Med. Chem.* **2005**, *48*, 5448.
8. Kirchmair, J.; Laggner, C.; Wolber, G.; Langer, T. *J. Chem. Inf. Model.* **2005**, *45*, 422.
9. Stahl, M.; Guba, W.; Kansy, M. *Drug Discovery Today* **2006**, *11*, 326.
10. Siedlecki, P.; Boy, R. G.; Comagic, S.; Schirrmacher, R.; Wiessler, M.; Zielenkiewicz, P.; Suhai, S.; Lyko, F. *Biochem. Biophys. Res. Commun.* **2003**, *306*, 558.
11. Siedlecki, P.; Boy, R. G.; Musch, T.; Brueckner, B.; Suhai, S.; Lyko, F.; Zielenkiewicz, P. *J. Med. Chem.* **2005**, *49*, 678.
12. Moustakas, D.; Lang, P.; Pegg, S.; Pettersen, E.; Kuntz, I.; Brooijmans, N.; Rizzo, R. *J. Comput. Aided Mol. Des.* **2006**, *20*, 601.
13. Medina-Franco, J.; López-Vallejo, F.; Kuck, D.; Lyko, F. *Mol. Divers.* in press [Epub ahead of print].
14. de Ruijter, A. J. M.; van Gennip, A. H.; Caron, H. N.; Kemp, S.; van Kuilenburg, A. B. P. *Biochem. J.* **2003**, *370*, 737.
15. Hodawadekar, S. C.; Marmorstein, R. *Oncogene* **2007**, *26*, 5528.
16. Zhang, Y.; Fang, H.; Jiao, J.; Xu, W. *Curr. Med. Chem.* **2008**, *15*, 2840.
17. Bressi, J. C.; Jennings, A. J.; Skene, R.; Wu, Y.; Melkus, R.; Jong, R. D.; O'Connell, S.; Grimshaw, C. E.; Navre, M.; Gangloff, A. R. *Bioorg. Med. Chem. Lett.* **2010**, *20*, 3142.
18. Massa, S.; Mai, A.; Sbardella, G.; Esposito, M.; Ragno, R.; Loidl, P.; Brosch, G. *J. Med. Chem.* **2001**, *44*, 2069.
19. Van Ommeslaeghe, K.; Elaut, G.; Brecx, V.; Papeleu, P.; Iterbeke, K.; Geerlings, P.; Tourwé, D.; Rogiers, V. *Bioorg. Med. Chem. Lett.* **2003**, *13*, 1861.
20. Wang, D.-F.; Wiest, O.; Helquist, P.; Lan-Hargest, H.-Y.; Wiech, N. L. *J. Med. Chem.* **2004**, *47*, 3409.
21. Lu, Q.; Wang, D.-S.; Chen, C.-S.; Hu, Y.-D.; Chen, C.-S. *J. Med. Chem.* **2005**, *48*, 5530.
22. Rodriquez, M.; Terracciano, S.; Cini, E.; Settembrini, G.; Bruno, I.; Bifulco, G.; Taddei, M.; Gomez-Paloma, L. *Angew. Chem., Int. Ed.* **2006**, *45*, 423.
23. Maulucci, N.; Chini, M. G.; Di Micco, S.; Izzo, I.; Cafaro, E.; Russo, A.; Gallinari, P.; Paolini, C.; Nardi, M. C.; Casapullo, A.; Riccio, R.; Bifulco, G.; De Riccardis, F. *J. Am. Chem. Soc.* **2007**, *129*, 3007.
24. Liu, T.; Kapustin, G.; Etzkorn, F. A. *J. Med. Chem.* **2007**, *50*, 2003.
25. Di Micco, S.; Terracciano, S.; Bruno, I.; Rodriquez, M.; Riccio, R.; Taddei, M.; Bifulco, G. *Bioorg. Med. Chem.* **2008**, *16*, 8635.
26. Chen, P. C.; Patil, V.; Guerrant, W.; Green, P.; Oyelere, A. K. *Bioorg. Med. Chem.* **2008**, *16*, 4839.
27. Grolla, A. A.; Podestà, V.; Chini, M. G.; Di Micco, S.; Vallario, A.; Genazzani, A. A.; Canonico, P. L.; Bifulco, G.; Tron, G. C.; Sorba, G.; Pirali, T. *J. Med. Chem.* **2009**, *52*, 2776.
28. Butler, K. V.; Kalin, J.; Brochier, C.; Vistoli, G.; Langley, B.; Kozikowski, A. P. *J. Am. Chem. Soc.* **2010**, *132*, 10842.
29. Lavoie, R.; Bouchain, G.; Frechette, S.; Woo, S. H.; Khalil, E. A.; Leit, S.; Fournel, M.; Yan, P. T.; Trachy-Bourget, M.-C.; Beaulieu, C.; Li, Z.; Besterman, J.; Delorme, D. *Bioorg. Med. Chem. Lett.* **2001**, *11*, 2847.
30. Remiszewski, S. W.; Sambucetti, L. C.; Atadja, P.; Bair, K. W.; Cornell, W. D.; Green, M. A.; Howell, K. L.; Jung, M.; Kwon, P.; Trogani, N.; Walker, H. *J. Med. Chem.* **2002**, *45*, 753.
31. Mai, A.; Massa, S.; Ragno, R.; Cerbara, I.; Jesacher, F.; Loidl, P.; Brosch, G. *J. Med. Chem.* **2003**, *46*, 512.
32. Park, H.; Lee, S. *J. Comput. Aided Mol. Des.* **2004**, *18*, 375.
33. Wang, D.-F.; Helquist, P.; Wiech, N. L.; Wiest, O. *J. Med. Chem.* **2005**, *48*, 6936.
34. Kim, H. M.; Hong, S. H.; Kim, M. S.; Lee, C. W.; Kang, J. S.; Lee, K.; Park, S.-K.; Han, J. W.; Lee, H. Y.; Choi, Y.; Kwon, H. J.; Han, G. *Bioorg. Med. Chem. Lett.* **2007**, *17*, 6234.
35. Witter, D. J.; Harrington, P.; Wilson, K. J.; Chenard, M.; Fleming, J. C.; Haines, B.; Kral, A. M.; Secrist, J. P.; Miller, T. A. *Bioorg. Med. Chem. Lett.* **2008**, *18*, 726.
36. Moradei, O. M.; Mallais, T. C.; Frechette, S.; Paquin, I.; Tessier, P. E.; Leit, S. M.; Fournel, M.; Bonfils, C.; Trachy-Bourget, M.-C.; Liu, J.; Yan, T. P.; Lu, A.-H.; Rahil, J.; Wang, J.; Lefebvre, S.; Li, Z.; Vaisburg, A. F.; Besterman, J. M. *J. Med. Chem.* **2007**, *50*, 5543.
37. Schäfer, S.; Saunders, L.; Eliseeva, E.; Velena, A.; Jung, M.; Schwienhorst, A.; Strasser, A.; Dickmanns, A.; Ficner, R.; Schlimme, S.; Sippl, W.; Verdin, E.; Jung, M. *Bioorg. Med. Chem.* **2008**, *16*, 2011.
38. Yan, C.; Xiu, Z.; Li, X.; Li, S.; Hao, C.; Teng, H. *Proteins* **2008**, *73*, 134.
39. Mukherjee, P.; Pradhan, A.; Shah, F.; Tekwani, B. L.; Avery, M. A. *Bioorg. Med. Chem.* **2008**, *16*, 5254.
40. Weerasinghe, S. V. W.; Estiu, G.; Wiest, O.; Pflum, M. K. H. *J. Med. Chem.* **2008**, *51*, 5542.
41. Estiu, G.; West, N.; Mazitschek, R.; Greenberg, E.; Bradner, J. E.; Wiest, O. *Bioorg. Med. Chem.* **2010**, *18*, 4103.
42. Estiu, G.; Greenberg, E.; Harrison, C. B.; Kwiatkowski, N. P.; Mazitschek, R.; Bradner, J. E.; Wiest, O. *J. Med. Chem.* **2008**, *51*, 2898.

43. Schäfer, S.; Saunders, L.; Schlimme, S.; Valkov, V.; Wagner, J.; Kratz, F.; Sippl, W.; Verdin, E.; Jung, M. *ChemMedChem* **2009**, *4*, 283.
44. Wang, D.-F.; Wiest, O.; Helquist, P.; Lan-Hargest, H.-Y.; Wiech, N. L. *Bioorg. Med. Chem. Lett.* **2004**, *14*, 707.
45. Xie, A.; Liao, C.; Li, Z.; Ning, Z.; Hu, W.; Lu, X.; Shi, L.; Zhou, J. *Curr. Med. Chem.: Anti-Cancer Agents* **2004**, *4*, 273.
46. Eikel, D.; Lampen, A.; Nau, H. *Chem. Res. Toxicol.* **2006**, *19*, 272.
47. Guo, Y.; Xiao, J.; Guo, Z.; Chu, F.; Cheng, Y.; Wu, S. *Bioorg. Med. Chem.* **2005**, *13*, 5424.
48. Juvale, D. C.; Kulkarni, V. V.; Deokar, H. S.; Wagh, N. K.; Padhye, S. B.; Kulkarni, V. M. *Org. Biomol. Chem.* **2006**, *4*, 2858.
49. Ragno, R.; Simeoni, S.; Valente, S.; Massa, S.; Mai, A. *J. Chem. Inf. Model.* **2006**, *46*, 1420.
50. Ragno, R.; Simeoni, S.; Rotili, D.; Caroli, A.; Botta, G.; Brosch, G.; Massa, S.; Mai, A. *Eur. J. Med. Chem.* **2008**, *43*, 621.
51. Tang, H.; Wang, X. S.; Huang, X.-P.; Roth, B. L.; Butler, K. V.; Kozikowski, A. P.; Jung, M.; Tropsha, A. *J. Chem. Inf. Model.* **2009**, *49*, 461.
52. Stahura, F. L.; Bajorath, J. *Curr. Pharm. Des.* **2005**, *11*, 1189.
53. Leach, A.; Shoichet, B.; Peishoff, C. *J. Med. Chem.* **2006**, *49*, 5851.
54. Waszkowycz, B. *Drug Discovery Today* **2008**, *13*, 219.
55. Klebe, G. *Drug Discovery Today* **2006**, *11*, 580.
56. Liebeschuetz, J. *J. Comput. Aided Mol. Des.* **2008**, *22*, 229.
57. Irwin, J. J. *J. Comput. Aided Mol. Des.* **2008**, *22*, 193.
58. Good, A.; Oprea, T. *J. Comput. Aided Mol. Des.* **2008**, *22*, 169.
59. Cross, J.; Thompson, D.; Rai, B.; Baber, C.; Fan, K.; Hu, Y.; Humblet, C. *J. Chem. Inf. Model.* **2009**, *49*, 1455.
60. Tame, J. *J. Comput. Aided Mol. Des.* **2005**, *19*, 445.
61. Kitchen, D. B.; Decornez, H.; Furr, J. R.; Bajorath, J. *Nat. Rev. Drug Discovery* **2004**, *3*, 935.
62. Hawkins, P.; Warren, G.; Skillman, A.; Nicholls, A. *J. Comput. Aided Mol. Des.* **2008**, *22*, 179.
63. Price, S.; Bordogna, W.; Bull, R. J.; Clark, D. E.; Crackett, P. H.; Dyke, H. J.; Gill, M.; Harris, N. V.; Gorski, J.; Lloyd, J.; Lockey, P. M.; Mullett, J.; Roach, A. G.; Roussel, F.; White, A. B. *Bioorg. Med. Chem. Lett.* **2007**, *17*, 370.
64. FlexE, BiosolveIT, St. Augustin, Germany.
65. Park, H.; Kim, S.; Kim, Y.; Lim, S. J. *ChemMedChem* **2010**, *5*, 591.
66. Chen, Y.-D.; Jiang, Y.-J.; Zhou, J.-W.; Yu, Q.-S.; You, Q.-D. *J. Mol. Graphics Model.* **2008**, *26*, 1160.
67. Ortore, G.; Colo, F. D.; Martinelli, A. *J. Chem. Inf. Model.* **2009**, *49*, 2774.
68. Vadivelan, S.; Sinha, B. N.; Rambabu, G.; Boppana, K.; Jagarlapudi, S. A. R. P. *J. Mol. Graphics Model.* **2008**, *26*, 935.
69. Sanders, B. D.; Jackson, B.; Marmorstein, R. *Biochim. Biophys. Acta, Proteins Proteomics* **2010**, *1804*, 1604.
70. Schuetz, A.; Min, J.; Antoshenko, T.; Wang, C.-L.; Allali-Hassani, A.; Dong, A.; Loppnau, P.; Vedadi, M.; Bochkarev, A.; Sternglanz, R.; Plotnikov, A. N. *Structure* **2007**, *15*, 377.
71. Sanders, B. D.; Zhao, K.; Slama, J. T.; Marmorstein, R. *Mol. Cell* **2007**, *25*, 463.
72. Trapp, J.; Meier, R.; Hongwiset, D.; Kassack, M.; Sippl, W.; Jung, M. *ChemMedChem* **2007**, *2*, 1419.
73. Neugebauer, R. C.; Sippl, W.; Jung, M. *Curr. Pharm. Des.* **2008**, *14*, 562.
74. Trapp, J.; Jochum, A.; Meier, R.; Saunders, L.; Marshall, B.; Kunick, C.; Verdin, E.; Goekjian, P.; Sippl, W.; Jung, M. *J. Med. Chem.* **2006**, *49*, 7307.
75. Tervo, A. J.; Kyrylenko, S.; Niskanen, P.; Salminen, A.; Leppänen, J.; Nyrönen, T. H.; Järvinen, T.; Poso, A. *J. Med. Chem.* **2004**, *47*, 6292–6298.
76. UNITY, Tripos International, St. Louis, USA.
77. Crivori, P.; Cruciani, G.; Carrupt, P.-A.; Testa, B. *J. Med. Chem.* **2000**, *43*, 2204–2216.
78. GOLD, Cambridge Crystallographic Data Centre, Cambridge, UK.
79. Huhtiniemi, T.; Suuronen, T.; Rinne, V. M.; Wittekindt, C.; Lahtela-Kakkonen, M.; Jarho, E.; Wallén, E. A. A.; Salminen, A.; Poso, A.; Leppänen, J. *J. Med. Chem.* **2008**, *51*, 4377.
80. Kiviranta, P. H.; Leppänen, J.; Kyrylenko, S.; Salo, H. S.; Lahtela-Kakkonen, M.; Tervo, A. J.; Wittekindt, C.; Suuronen, T.; Kuusisto, E.; Järvinen, T.; Salminen, A.; Poso, A.; Wallén, E. A. A. *J. Med. Chem.* **2006**, *49*, 7907.
81. Tervo, A. J.; Suuronen, T.; Kyrylenko, S.; Kuusisto, E.; Kiviranta, P. H.; Salminen, A.; Leppänen, J.; Poso, A. *J. Med. Chem.* **2006**, *49*, 7239.
82. Outeiro, T. F.; Kontopoulos, E.; Altmann, S. M.; Kufareva, I.; Strathearn, K. E.; Amore, A. M.; Volk, C. B.; Maxwell, M. M.; Rochet, J.-C.; McLean, P. J.; Young, A. B.; Abagyan, R.; Feany, M. B.; Hyman, B. T.; Kazantsev, A. G. *Science* **2007**, *317*, 516.
83. Abagyan, R.; Totrov, M.; Kuznetsov, D. *J. Comput. Chem.* **1994**, *15*, 488.
84. Neugebauer, R. C.; Uchiechowska, U.; Meier, R.; Hruby, H.; Valkov, V.; Verdin, E.; Sippl, W.; Jung, M. *J. Med. Chem.* **2008**, *51*, 1203.
85. Medda, F.; Russell, R. J. M.; Higgins, M.; McCarthy, A. R.; Campbell, J.; Slawin, A. M. Z.; Lane, D. P.; Lain, S.; Westwood, N. J. *J. Med. Chem.* **2009**, *52*, 2673.
86. Heltweg, B.; Gatbonton, T.; Schuler, A. D.; Posakony, J.; Li, H.; Goehle, S.; Kollipara, R.; DePinho, R. A.; Gu, Y.; Simon, J. A.; Bedalov, A. *Cancer Res.* **2006**, *66*, 4368.
87. Wang, J.; Wolf, R. M.; Caldwell, J. W.; Kollman, P. A.; Case, D. A. *J. Comput. Chem.* **2004**, *25*, 1157.
88. Lin, Y.; Fletcher, C. M.; Zhou, J.; Allis, C. D.; Wagner, G. *Nature* **1999**, *400*, 86.
89. Liu, X.; Wang, L.; Zhao, K.; Thompson, P. R.; Hwang, Y.; Marmorstein, R.; Cole, P. A. *Nature* **2008**, *451*, 846.
90. Trievel, R. C.; Rojas, J. R.; Sterner, D. E.; Venkataramani, R. N.; Wang, L.; Zhou, J.; Allis, C. D.; Berger, S. L.; Marmorstein, R. *Proc. Natl. Acad. Sci. U.S.A.* **1999**, *96*, 8931.
91. Bowers, E. M.; Yan, G.; Mukherjee, C.; Orry, A.; Wang, L.; Holbert, M. A.; Crump, N. T.; Hazzalin, C. A.; Liszczak, G.; Yuan, H.; Larocca, C.; Saldanha, S. A.; Abagyan, R.; Sun, Y.; Meyers, D. J.; Marmorstein, R.; Mahadevan, L. C.; Alani, R. M.; Cole, P. A. *Chem. Biol.* **2010**, *17*, 471.
92. von Wantoch Rekowski, M.; Giannis, A. *Epigenetic Targets in Drug Discovery*;; Wiley-VCH Verlag GmbH & Co. KGaA, 2009. pp 243–250.
93. Bhaumik, S. R.; Smith, E.; Shilatifard, A. *Nat. Struct. Mol. Biol.* **2007**, *14*, 1008.
94. Chang, Y.; Zhang, X.; Horton, J. R.; Upadhyay, A. K.; Spannhoff, A.; Liu, J.; Snyder, J. P.; Bedford, M. T.; Cheng, X. *Nat. Struct. Mol. Biol.* **2009**, *16*, 312.
95. Zhang, X.; Zhou, L.; Cheng, X. *EMBO J.* **2000**, *19*, 3509.
96. Zhang, X.; Cheng, X. *Structure* **2003**, *11*, 509.
97. Ragno, R.; Simeoni, S.; Castellano, S.; Vicidomini, C.; Mai, A.; Caroli, A.; Tramontano, A.; Bonaccini, C.; Trojer, P.; Bauer, I.; Brosch, G.; Sbardella, G. *J. Med. Chem.* **2007**, *50*, 1241.
98. Baroni, M.; Costantino, G.; Cruciani, G.; Riganelli, D.; Valigi, R.; Clementi, S. *Quant. Struct.-Act. Relat.* **1993**, *12*, 9.
99. Mai, A.; Valente, S.; Cheng, D.; Perrone, A.; Ragno, R.; Simeoni, S.; Sbardella, G.; Brosch, G.; Nebbioso, A.; Conte, M.; Altucci, L.; Bedford, M. *ChemMedChem* **2007**, *2*, 987.
100. Spannhoff, A.; Heinke, R.; Bauer, I.; Trojer, P.; Metzger, E.; Gust, R.; Schüle, R.; Brosch, G.; Sippl, W.; Jung, M. *J. Med. Chem.* **2007**, *50*, 2319.
101. Heinke, R.; Spannhoff, A.; Meier, R.; Trojer, P.; Bauer, I.; Jung, M.; Sippl, W. *ChemMedChem* **2009**, *4*, 69.
102. Spannhoff, A.; Machmur, R.; Heinke, R.; Trojer, P.; Bauer, I.; Brosch, G.; Schüle, R.; Hanefeld, W.; Sippl, W.; Jung, M. *Bioorg. Med. Chem. Lett.* **2007**, *17*, 4150.
103. Kubicek, S.; O'Sullivan, R. J.; August, E. M.; Hickey, E. R.; Zhang, Q.; Teodoro; Miguel, L.; Rea, S.; Mechtler, K.; Kowalski, J. A.; Homon, C. A.; Kelly, T. A.; Jenuwein, T. *Mol. Cell* **2007**, *25*, 473.
104. Cheng, D.; Yadav, N.; King, R. W.; Swanson, M. S.; Weinstein, E. J.; Bedford, M. T. *J. Biol. Chem.* **2004**, *279*, 23892.
105. Mason, J. S.; Morize, I.; Menard, P. R.; Cheney, D. L.; Hulme, C.; Labaudiniere, R. F. *J. Med. Chem.* **1999**, *42*, 3251.
106. Zhang, X.; Yang, Z.; Khan, S. I.; Horton, J. R.; Tamaru, H.; Selker, E. U.; Cheng, X. *Mol. Cell* **2003**, *12*, 177.
107. Shi, Y.; Lan, F.; Matson, C.; Mulligan, P.; Whetstine, J. R.; Cole, P. A.; Casero, R. A.; Shi, Y. *Cell* **2004**, *119*, 941.
108. Metzger, E.; Wissmann, M.; Yin, N.; Muller, J. M.; Schneider, R.; Peters, A. H. F. M.; Gunther, T.; Buettner, R.; Schule, R. *Nature* **2005**, *437*, 436.
109. Tsukada, Y.-I.; Fang, J.; Erdjument-Bromage, H.; Warren, M. E.; Borchers, C. H.; Tempst, P.; Zhang, Y. *Nature* **2006**, *439*, 811.
110. Wang, G. G.; Allis, C. D.; Chi, P. *Trends Mol. Med.* **2007**, *13*, 363.
111. Mantri, M.; Krojer, T.; Bagg, E. A.; Webby, C. J.; Butler, D. S.; Kochan, G.; Kavanagh, K. L.; Oppermann, U.; McDonough, M. A.; Schofield, C. J. *J. Mol. Biol.* **2010**, *401*, 211.
112. Rose, N. R.; Woon, E. C. Y.; Kingham, G. L.; King, O. N. F.; Mecinovic, J.; Clifton, I. J.; Ng, S. S.; Talib-Hardy, J.; Oppermann, U.; McDonough, M. A.; Schofield, C. J. *J. Med. Chem.* **2010**, *53*, 1810.
113. Rose, N. R.; Ng, S. S.; Mecinović, J.; Liénard, B. M.; Bello, S. H.; Sun, Z.; McDonough, M. A.; Oppermann, U.; Schofield, C. J. *J. Med. Chem.* **2008**, *51*, 7053.